Statistics of subthreshold neuronal voltage fluctuations due to conductance-based synaptic shot noise

Magnus J. E. Richardson[a)]
École Polytechnique Fédérale de Lausanne (EPFL), Laboratory of Computational Neuroscience, School of Computer and Communication Sciences and Brain Mind Institute, CH-1015 Lausanne, Switzerland and Warwick Systems Biology Centre, University of Warwick, Coventry CV4 7AL, United Kingdom

Wulfram Gerstner[b)]
École Polytechnique Fédérale de Lausanne (EPFL), Laboratory of Computational Neuroscience, School of Computer and Communication Sciences and Brain Mind Institute, CH-1015 Lausanne, Switzerland

(Received 20 January 2006; accepted 18 April 2006; published online 30 June 2006)

Neurons in the central nervous system, and in the cortex in particular, are subject to a barrage of pulses from their presynaptic populations. These synaptic pulses are mediated by conductance changes and therefore lead to increases or decreases of the neuronal membrane potential with amplitudes that are dependent on the voltage: synaptic noise is multiplicative. The statistics of the membrane potential are of experimental interest because the measurement of a single subthreshold voltage can be used to probe the activity occurring across the presynaptic population. Though the interpulse interval is not always significantly smaller than the characteristic decay time of the pulses, and so the fluctuations have the nature of shot noise, the majority of results available in the literature have been calculated in the diffusion limit, which is valid for high-rate pulses. Here the effects that multiplicative conductance noise and shot noise have on the voltage fluctuations are examined. It is shown that both these aspects of synaptic drive sculpt high-order features of the subthreshold voltage distribution, such as the skew. It is further shown that the diffusion approximation can only capture the effects arising from the multiplicative conductance noise, predicting a negative voltage skew for excitatory drive. Exact results for the full dynamics are derived from a master-equation approach, predicting positively skewed distributions with long tails in voltage ranges typical for action potential generation. It is argued that, although the skew is a high-order feature of subthreshold voltage distributions, the increased probability of reaching firing threshold suggests a potential role for shot noise in shaping the neuronal transfer function. [DOI: 10.1063/1.2203409]

Neurons communicate via their axons by the activation of excitatory or inhibitory synapses that act to increase or decrease the voltage of the target neuron. Cortical neurons receive many thousands of connections from active presynaptic cells and are therefore subject to a highly fluctuating drive. The statistics of the resulting voltage contains much information on the state of the presynaptic population and has been used experimentally as a probe of network activity. However, to properly interpret the voltage fluctuations, accurate models of the effect of synaptic drive on the subthreshold voltage are required. Two important aspects of synaptic input are (1) that it is mediated by multiplicative conductance noise, and (2) that the individual pulses can be sufficiently well separated such that it constitutes shot noise. The latter effect means that a common approach, which treats the fluctuations in the diffusion limit, is not always accurate. Here the case of multiplicative shot noise will be addressed and the weaknesses and strengths of the diffusion approximation identified.

I. INTRODUCTION

The code that neurons use to communicate to one another in the cortex is a subject of intense research. One of the difficulties of inferring the code is that it is distributed over populations of many thousands of neurons, as evidenced in the motor cortex in the population vectors[1] that code for hand position or muscle action.[2] One method of indirectly measuring the activity of a population of neurons is by using the fluctuating voltage of a neuron embedded in an active network as a probe:[3] given a model of the effect of the barrage of synaptic pulses on the neuronal voltage, the resulting statistics can be used to infer the state of the presynaptic network. As well as the response of the neuron to its drive, the form of the voltage fluctuations also determines whether an action potential will be output from a neuron. Hence, the accurate modeling of the effect of presynaptic pulses on the subthreshold potential of neurons[4–6] is of great interest to experimental measures of network activity and to the under-

[a)]Electronic mail: Magnus.Richardson@warwick.ac.uk
[b)]Electronic mail: Wulfram.Gerstner@epfl.ch

standing of the neuron as a basic input-output unit of the central nervous system.

A fundamental model of the electrical response of driven cells was introduced by Lapicque[7] and featured a passive decay of the voltage due to the capacitance and leak conductance of the cellular membrane. Later, Stein introduced a model featuring a synaptic drive modeled as a conductance change,[8] following which the effects of stochastic, conductance-based synaptic drive on membrane potential fluctuations began to be extensively studied.[9–12] These initial studies typically treated the fluctuating drive in the diffusion limit and were principally interested in the statistics of the interspike interval distribution of the outgoing spikes generated by the neuron, rather than the voltage distribution itself. Since the early theoretical work, many experimental studies have directly probed the conductance change due to the synaptic drive[13–17] and have shown that the conductance can be as much as five times higher than that of a neuron in an inactive network. That the synaptic conductance change is dominant has led to renewed theoretical interest in the synaptic drive, particularly on the nonlinear effect that the conductance change has on the gain of neurons.[18–24]

More recently, studies have directed their attention toward the statistics of the subthreshold voltage distribution. A solution was recently proposed[25] for the case of filtered synaptic drive (in which the synaptic drive was modeled by two Ornstein-Uhlenbeck processes with distinct time constants for excitatory and inhibitory synapses). However, doubt has been cast[6,26–28] on the correctness of the approach used. Though an exact solution for the case of filtered synaptic drive remains illusive, a number of approximation schemes are now available.[6,28,29]

The effects of another feature of synaptic drive, shot noise, have been comparatively less studied. However, it has been included in the context of the interspike interval distribution,[30] incorporated into numerical schemes for calculating the firing rate of neuronal populations,[31] considered in relation to stochastic resonance in neurons,[32] included in an analysis of the effects of correlations in the presynaptic population,[33] and a perturbative approach has recently been developed for the case of a filtered synaptic shot noise.[6]

Here, the effect of multiplicative, conductance-based shot noise on the voltage statistics of neurons receiving delta-pulse synapses is examined in detail. After defining the model to be analyzed, the weakness of the diffusion approximation in the analysis of subthreshold voltage fluctuations is first identified and the full master equation introduced. In this Focus Article both established results and new results, specifically for the exact forms for the mean, variance, and skew for arbitrary synaptic amplitude distributions, are presented. Though the analysis is restricted to the case of subthreshold voltage fluctuations, the implications of some of the results for the firing rate of neurons are considered in Sec. V.

II. THE MODEL

The electrical properties of the neuronal membrane can be derived by modeling it as a capacitance C in parallel with a passive leak current of constant conductance g_L and a synaptic current I_{syn} composed of fluctuating conductances. The ratio of the capacitance and the leak conductance $\tau_L = C/g_L$ defines the passive time constant of the neuron. This sets the scale for the relaxation of the cellular voltage following any disturbance that takes it away from its equilibrium value E_L. With these definitions, the capacitive charging of the cell membrane can be seen to obey the following equation:

$$C\frac{dV}{dt} = -g_L(V - E_L) - I_{\mathrm{syn}}(t), \tag{1}$$

from which the time course of the voltage $V(t)$ at time t can be derived as a function of the synaptic current. It should be noted that no spike-generating currents have been included in the voltage equation. This is in keeping with the aim here of analyzing the statistics of the subthreshold voltage of cells driven by synapses with finite-sized amplitudes. This scenario is directly relevant to experiments that use a hyperpolarized neuron as a probe for the presynaptic network activity.[3]

A. Synaptic shot noise

The synaptic current I_{syn} can be modeled[8] as comprising two fluctuating components: an excitatory conductance $g_e(t)$ that acts to depolarize the neuron by bringing its voltage closer to the reversal potential $E_e = 0$ mV for excitation, and an inhibitory conductance $g_i(t)$ that acts to hyperpolarize its voltage by bringing it closer to the reversal potential $E_i = -75$ mV for inhibition. The net current can be written as a sum of these two components:

$$I_{\mathrm{syn}}(t) = g_e(t)(V - E_e) + g_i(t)(V - E_i). \tag{2}$$

The conductances themselves are activated by a barrage of presynaptic pulses, each of which is modeled here as causing a delta-pulse conductance of strength $a_e C$, where from now on excitation will be used as an example with similar statements for inhibition following by analogy. Thus, for excitation,

$$g_e(t) = a_e C \sum_{\{t_e\}} \delta(t - t_e), \tag{3}$$

where $\{t_e\}$ is the set of excitatory presynaptic pulse times that follow a Poisson process with a constant rate $\mathcal{R}_e$.

Modeling the conductance changes as a series of impulses is an approximation; synaptic channels have characteristic time scales for inactivation (about 3 ms for excitation and 10 ms for inhibition). However, for the purposes of this paper, which concentrates on the shot-noise aspect of the drive, this filtering will be ignored (the reader is directed elsewhere[6] for a perturbative treatment of filtered, conductance-based shot noise). It should also be noted that the case of non-Poissonian drive (see, for example, Ref. 34) is beyond the scope of this article (see Ref. 35 for a treatment of temporally correlated input in the diffusion approximation).

On inserting the form for the synaptic drive (2) into the voltage equation (1), dividing by $V - E_e$, and integrating over a short period of time that includes a single excitatory input, it is seen that the membrane voltage jumps from V to $V + \Delta$ with

$$\Delta = (E_e - V)(1 - e^{-a_e}) = (E_e - V)b_e, \tag{4}$$

where the effective amplitude b_e has been introduced. This form of the voltage jump follows the usual rules of calculus and is the same as that chosen in Ref. 31.

1. Stratonovich versus Itô stochastic calculus

It is possible to make a different choice from the update rule (4) by retarding the multiplicative voltage prefactor of the synaptic drive in Eq. (2). If such a choice is made, the driving term for excitation, for example, becomes $g_e(t)[V(t-\epsilon)-E_e]$, where ϵ is a positive infinitesimal. The update rule corresponding to (4) would then be $\Delta=(E_e-V)a_e$ instead. In the diffusion limit (to be discussed in Sec. III), this choice would correspond to the Itô form of stochastic calculus, whereas the choice (4) corresponds to the Stratonovich form.[37] Throughout this paper it will be the Stratonovich form that is chosen. However, when a_e is small, the two formulations become practically indistinguishable. It can be noted that by making the replacement $b_e \to a_e$ the Itô formulation is obtained.

2. Numerical simulations of synaptic shot noise

A discretized form of the voltage equation (1) can be used for Monte Carlo simulations of the dynamics. For the purposes of this paper a simple forward Euler scheme was found to be adequate, with an integration time step $\Delta_t = 50\ \mu$s, or smaller, used. The discrete-time dynamics for the voltage V_k at time step $t_k = k\Delta_t$ can be written, following the rule in Eq. (4), as

$$V_{k+1} = V_k + \frac{\Delta_t}{\tau_L}(E_L - V_k) + e_k b_e (E_e - V_k) + i_k b_i (E_i - V_k), \tag{5}$$

where e_k, i_k are integers drawn from Poisson distributions with means $\mathcal{R}_e\Delta_t$, $\mathcal{R}_i\Delta_t$. This is an approximation to Poissonian statistics, valid to order Δ_t and therefore consistent with this first-order Euler scheme: a small Δ_t must be chosen (as specified above) for accuracy such that e_k or i_k infrequently take a value of greater than unity . It should be noted that an exact integration scheme can be implemented by calculating the time to the next event using the Poissonian interval distribution—this method is discussed in Ref. 36.

III. THE DIFFUSION APPROXIMATION

A standard approach for dealing with Poissonian shot noise is to take the diffusion limit. In the context of a fluctuating subthreshold voltage this approach becomes accurate in the limit in which many excitatory and inhibitory synaptic pulses arrive within the relaxation time τ_L of the dynamics, i.e., that $\mathcal{R}_e\tau_L \gg 1$ and $\mathcal{R}_i\tau_L \gg 1$. When this holds, the Poissonian fluctuations are well approximated by a Gaussian process. In this section the diffusion approximation of the voltage dynamics first will be obtained and the corresponding Fokker-Planck equation for the probability distribution derived. The predictions of this approximation will then be compared to the full dynamics and its weaknesses identified.

To obtain the diffusion approximation, the aim is to approximate the stochastic synaptic current given in Eqs. (2) and (3) by a Gaussian process of identical mean and variance. Using the excitatory conductance as an example, consider first the integration of this contribution to $I_{\rm syn}$ over a short time t_k to $t_{k+1}=t_k+\Delta_t$:

$$g_e(V - E_e) = \frac{1}{\Delta_t}\int_{t_k}^{t_{k+1}} dt C a_e \sum_{\{t_e\}} \delta(t - t_e)(V - E_e). \tag{6}$$

Finding the mean and variance of this quantity is complicated by the fact that a delta function multiplies the voltage under the integral. However, on combining the rule given in Eq. (4) with the voltage equation (1), the first two moments can be found to be

$$\langle g_e(V - E_e)\rangle = C\mathcal{R}_e b_e (V_k - E_e), \tag{7}$$

$$\mathrm{Var}[g_e(V - E_e)] = C^2\mathcal{R}_e b_e^2 (V_k - E_e)^2/\Delta_t, \tag{8}$$

where $V_k = V(t_k)$ is the value of the voltage before any inputs arrive (these equations nevertheless correspond to the Stratonovich form of stochastic calculus).

To keep the form of the dynamics unambiguous, the discrete form for the evolution will be written directly. To this end, it proves convenient to introduce an effective time constant τ and the drive-dependent equilibrium potential E:

$$\tau^{-1} = \tau_L^{-1} + \mathcal{R}_e b_e + \mathcal{R}_i b_i, \tag{9}$$

$$E = \tau(E_L\tau_L^{-1} + E_e\mathcal{R}_e b_e + E_i\mathcal{R}_i b_i). \tag{10}$$

In terms of these variables the discrete-time equation for the voltage can be written

$$V_{k+1} = V_k + \frac{\Delta_t}{\tau}(E - V_k) + \sqrt{\Delta_t[\mathcal{R}_e b_e^2 (E_e - V_k)^2 + \mathcal{R}_i b_i^2 (E_i - V_k)^2]}\,\psi_k, \tag{11}$$

where the two Gaussian processes for excitation and inhibition have been merged and ψ_k is a Gaussian random number of zero mean and unit variance drawn for each time step. This discrete evolution equation is a translation into Îto form of the true Stratonovich dynamics. The corresponding Fokker-Planck equation[37] for the diffusion-level voltage distribution $P_D(V)$ can be written

$$\frac{\partial}{\partial t}P_D = \frac{1}{2}\frac{\partial^2}{\partial V^2}[(\mathcal{R}_e b_e^2 (E_e - V)^2 + \mathcal{R}_i b_i^2 (E_i - V)^2)P_D] + \frac{1}{\tau}\frac{\partial}{\partial V}[(V - E)P_D]. \tag{12}$$

A brief technical point: to order a_e^2, a_i^2, this Fokker-Planck equation is identical to that which would be obtained directly for the Stratonovich formulation for the replacement $g_e = Ca_e[\mathcal{R}_e + \sqrt{\mathcal{R}_e}\xi_e(t)]$, where $\xi_e(t)$ is delta-correlated white noise.[26,37] However, as will be seen, the form used in Eq. (12) has the added advantage of giving the mean and variance of the voltage correct to all orders in a_e, a_i as expressed via b_e, b_i.

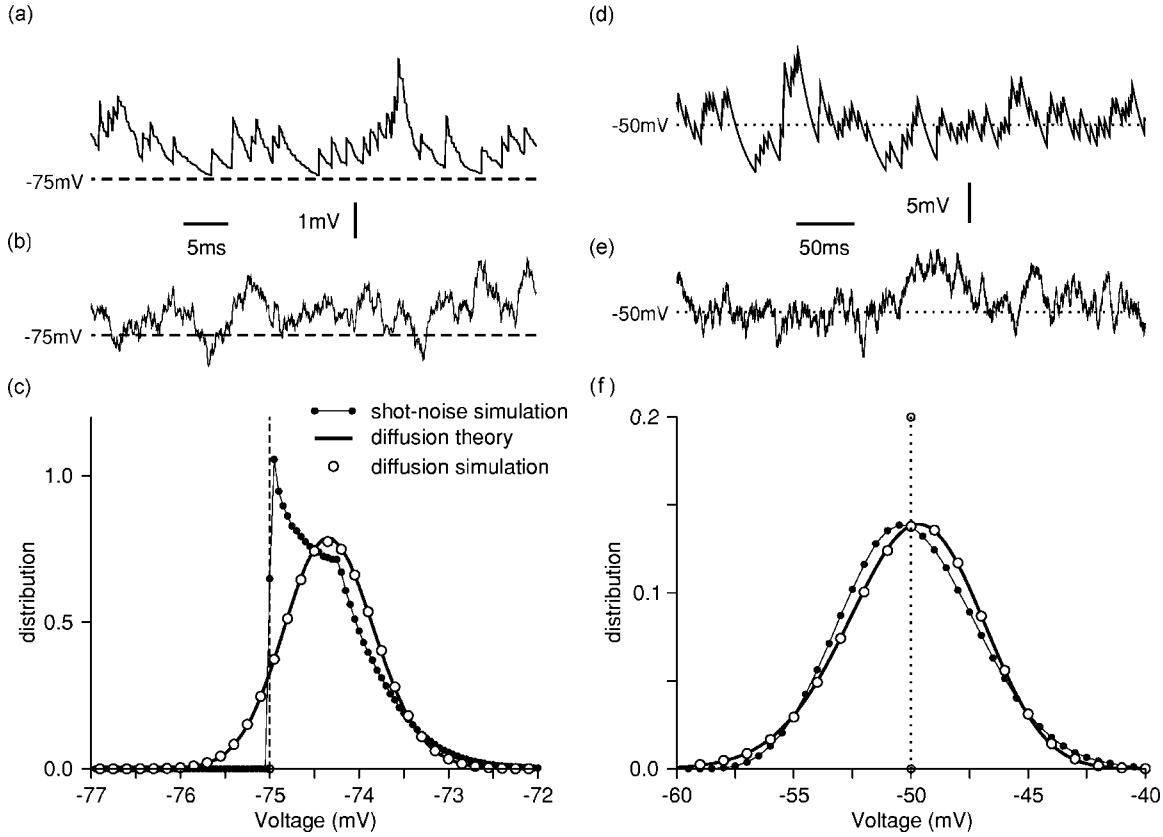

FIG. 1. Comparison of the shot-noise and diffusion-approximation voltage dynamics. (a)–(c) A case demonstrating the boundary error of the diffusion approximation: a neuron receiving both excitatory and strong inhibitory drive bringing it close to the inhibitory potential $E_i=-75$ mV, with a leak potential also set at $E_L=-75$ mV. (a) Shot-noise simulation of the dynamics. Between pulses the neuronal voltage relaxes to E_L. (b) Diffusion simulation using Eq. (11). Note that the voltage erroneously crosses the inhibitory reversal potential, which is not possible under the correct dynamics. (c) The steady-state shot-noise and diffusion-level voltage distributions. The diffusion approximation [simulation, Eq. (11); exact solution, Eq. (13)] gives a significant weight to the forbidden region below $E_i=E_L=-75$ mV. (d)–(f) A case demonstrating the skew error of the diffusion approximation: a neuron receiving excitatory drive only with a leak potential $E_L=-60$ mV. (d) Shot-noise simulation and (e) diffusion-level simulation. The average voltage E is -50 mV in both cases (dotted lines). (f) The shot-noise distribution is positively skewed (peak left of the average, tail to the right) whereas its diffusion approximation predicts a negative skew with the peak to the right of the average voltage. The parameters $\{\mathcal{R}_e, b_e, \mathcal{R}_i, b_i\}$ used for the drive were as follows: (a)–(c) {0.5, 0.01, 10, 0.05}, (d)–(f) {0.25, 0.04, 0, 0} with the rates given in kHz.

A. The diffusion-level voltage distribution

As stated earlier, the rates $\mathcal{R}_e$, $\mathcal{R}_i$ are steady and so, though the voltage has a dynamics, its statistics are stationary. The corresponding steady-state (i.e., setting $\partial_t P_D=0$) Fokker-Planck equation (12) is straightforward to solve[9,26] with the solution taking the following form:

$$
\begin{aligned}
&P_D \propto \exp[-AF(V)]/G(V),\\
&A = \frac{1}{\sqrt{\beta_e\beta_i}}\frac{1}{|E_e-E_i|}\frac{\beta_e\mathcal{E}_e+\beta_i\mathcal{E}_i}{\beta_e+\beta_i},\\
&F(V) = \arctan\left(\frac{\beta_e(V-E_e)+\beta_i(V-E_i)}{\sqrt{\beta_e\beta_i}|E_e-E_i|}\right),\\
&G(V) = [\beta_e(V-E_e)^2+\beta_i(V-E_i)^2]^{[1+1/2(\beta_e+\beta_i)]},
\end{aligned}
\tag{13}
$$

where the simplifying notation $\beta_e=\tau\mathcal{R}_e b_e^2/2$ and relative reversal potential $\mathcal{E}_e=E_e-E$ have been introduced (and similarly for the i, L subscripts).

It should be noted that the distribution predicted by the diffusion approximation is continuous over the voltage range. This is, however, not the case for the true shot-noise dynamics: if $E_L<E_e$, it is not possible for excitatory input to push the voltage over the reversal potential E_e for excitation (similarly, if the leak reversal E_L is chosen such that $E_i<E_L<E_e$, then the voltage would be bound between E_i and E_e). Hence the voltage should be bound by the leak and synaptic reversal potentials and the distribution should vanish outside this region.

That the diffusion approximation is not able to deal correctly with the reversal potential boundaries has been long recognized[12] and represents one of its weaknesses in its modeling of conductance-based drive (in this reference a number of alternative models to that considered here are discussed in detail, such as diffusion-level models that make the boundaries unreachable). An example of this is given in Figs. 1(a)–1(c). For the correct shot-noise dynamics the voltage is unable to cross the boundary for inhibition; the closer the voltage gets to E_i, the weaker the multiplicative inhibitory drive becomes. However, in the diffusion approximation, the excitatory noise is Gaussian (effectively predicting some negative conductances) and so causes the voltage to overlap into the forbidden zone below the inhibitory reversal poten-

tial. This effect can be seen clearly in simulations of the voltage time course in Fig. 1(b) well as in the distribution in Fig. 1(c).

B. The diffusion-level voltage moments

The mathematical form of the solution given in Eq. (13) for the diffusion-level distribution P_D does not provide for a transparent understanding of its form. A convenient way of classifying a distribution is via its moments, such as the mean and variance. For the diffusion-level distribution, such moments can be easily obtained by multiplying the Fokker-Planck equation and integrating over the voltage range. It proves convenient to measure the voltage as a difference from its mean E given in Eq. (10). On multiplying the steady-state form of Eq. (12) by v^m, where $v=(V-E)$, and integrating over this variable, the following recursion relation for the moments of the probability distribution is found:

$$0=\left(\frac{1}{2}(m-1)(\mathcal{R}_e b_e^2+\mathcal{R}_i b_i^2)-\frac{1}{\tau}\right)\langle v^m\rangle_D - (m-1)(\mathcal{R}_e b_e^2\mathcal{E}_e+R_i b_i^2\mathcal{E}_i)\langle v^{m-1}\rangle_D + \frac{1}{2}(m-1)(\mathcal{R}_e b_e^2\mathcal{E}_e^2+R_i b_i^2\mathcal{E}_i^2)\langle v^{m-2}\rangle_D, \tag{14}$$

where the D subscripts remind the reader that the average here is over the diffusion-level voltage distribution. By setting $m=1$, it is seen that the average voltage V is identical to E, i.e., $\langle v\rangle_D=0$. From the case of $m=2$, the diffusion-level voltage variance σ_D^2 is found to be

$$\sigma_D^2=\frac{\tau_L}{2}\frac{\mathcal{R}_e b_e^2\mathcal{E}_e^2+\mathcal{R}_i b_i^2\mathcal{E}_i^2}{1+\tau_L\mathcal{R}_e b_e(1-b_e/2)+\tau_L\mathcal{R}_i b_i(1-b_i/2)}. \tag{15}$$

Also of interest is how non-Gaussian the distribution is. The skew, defined as $\mathcal{S}=\langle v\rangle^3/\sigma^3$, provides one such measure and can be written in terms of the standard deviation σ_D by using Eq. (14) with $m=3$:

$$\mathcal{S}_D=-\frac{2\tau_L}{\sigma_D}\frac{\mathcal{R}_e b_e^2\mathcal{E}_e+\mathcal{R}_i b_i^2\mathcal{E}_i}{1+\mathcal{R}_e\tau_L b_e(1-b_e)+\mathcal{R}_i\tau_L b_i(1-b_i)}. \tag{16}$$

For both the variance and skew, the effective time constant τ [Eq. (9)] has been replaced by its form in terms of the passive time constant τ_L and the rates $\mathcal{R}_e$, $\mathcal{R}_i$.

To compare the diffusion-level form for the skew with simulation of the full model, a special case is considered in which inhibition is absent. In the limit of high-rate and small amplitudes, with $\tau_L\mathcal{R}_e b_e$ held constant so as to keep the average voltage E fixed, the skew can be written

$$\mathcal{S}_D\simeq-\sqrt{\frac{8\tau_L\mathcal{R}_e b_e^2}{1+\tau_L\mathcal{R}_e b_e}}\sim\sqrt{b_e} \tag{17}$$

and seen to be proportional to the root of b_e (note that this is the same for the standard deviation). For the case of the purely excitatory drive, the diffusion approximation predicts a skew that is always negative.

It is not surprising that in the extreme case near the reversal of inhibition [shown in Figs. 1(a)–1(c)] the skew predicted from the diffusion approximation will be inaccurate. However, even away from the inhibitory reversal the skew is given incorrectly by the diffusion approximation. In Figs. 1(d) and 1(e) an example is given for a neuron driven by an excitatory drive with a fluctuating voltage of average value −50 mV. As can be seen in the figure, the skew predicted by the diffusion approximation is negative with a value −0.23, whereas the distribution of voltages from the shot-noise simulation is positively skewed with a magnitude 0.23 (a mirror-image case was chosen). The difference between the true skew and its diffusion approximation is explored further in Fig. 2 as a function of b_e while $\tau_L\mathcal{R}_e b_e$ is again held constant. As can be seen, for the examples, the diffusion approximation is systematically in error in its estimation of the skew.

IV. ACCOUNTING FOR SHOT NOISE

The full shot-noise statistics will now be addressed. As an illustration, the case of a uniamplitude distribution of synaptic weights will be considered first and the master equation for the dynamics of the voltage distribution presented. As will be seen, it is possible also in this case to derive arbitrary moments of the voltage distribution; these will be compared to the mean, variance, and skew derived in the diffusion approximation. The link between the diffusion approximation and the full dynamics is then examined and a consistent expansion of the master equation provided. The use of the simple uniamplitude case (in the absence of inhibition) also allows for an analytical recursion solution[30,33,38] for the voltage distribution to be reviewed. The section closes with an analysis of the more general case in which the excitatory and inhibitory synaptic strengths take a range of values. The particular case of an exponential distribution of synaptic amplitudes is given as an example.

A. The master equation for shot-noise drive

In the previous section the Fokker-Planck equation was derived for the diffusion limit of high-rate synaptic pulses. A more general equation, the master equation, can be written down for the full probability density P that is valid for arbitrary rate pulses. This equation can be derived by considering an ensemble of equivalent neurons. There are three ways that neurons can enter a particular voltage range V to $V+\delta_V$: (1) from an excitatory jump into the range from some lower voltage; (2) from an inhibitory jump into the range from a higher voltage; and (3) by drifting in due to the leak term. Correspondingly, there are three analogous ways of leaving this voltage range. When the effects of these processes on the probability (proportion of neurons within the ensemble) of finding a neuron in this range are accounted for, the following equation is obtained:

$$\frac{\partial}{\partial t}P(V)=\mathcal{R}_e\left[\frac{1}{1-b_e}P\left(\frac{V-b_eE_e}{1-b_e}\right)-P(V)\right] + \mathcal{R}_i\left[\frac{1}{1-b_i}P\left(\frac{V-b_iE_i}{1-b_i}\right)-P(V)\right] + \frac{1}{\tau_L}\frac{\partial}{\partial V}[(V-E_L)P(V)]. \tag{18}$$

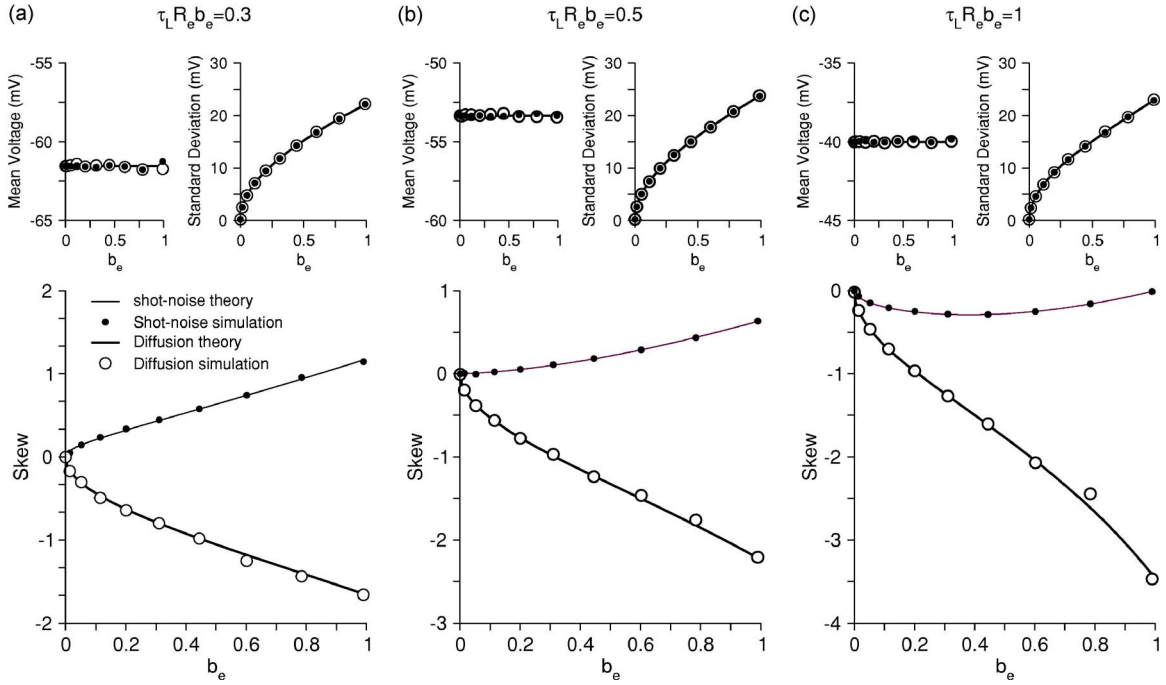

FIG. 2. Comparison of the voltage moments calculated for the shot-noise and diffusion-level dynamics. Three cases are considered for which $\tau_L \mathcal{R}_e b_e$ is held constant (marked on panels) while b_e is varied over its full range $\{0, 1\}$ in the absence of inhibition. In the upper panels, for all cases (a)–(c), it is seen that the diffusion-level mean, Eq. (10), and variance, Eq. (15) (here plotted in the form of the standard deviation), agree with the corresponding shot-noise moments derived from Eq. (19). The diffusion-level skew, Eq. (16), however, can be seen to be incorrect in comparison with the shot-noise form, Eq. (21), even in its expected range of validity for b_e small $\tau_L \mathcal{R}_e$ large. (a) Lower panel: the true skew is positive, whereas the diffusion approximation predicts a negative value. (c) Lower panel: both the shot-noise and diffusion-approximation skew are negative, but with different magnitudes. (b) Lower panel: the intermediate case. In all examples $E_L = -80$ mV and $\tau_L = 20$ ms.

This equation, written in a form where the probability current is explicit, has been used previously[30] in combination with a threshold for spike initiation to examine the interspike interval of neurons driven by conductance-based shot noise. An efficient numerical scheme for the solution of this equation has also been presented.[31]

B. Voltage moments of the master equation

The exact mean, variance, and skew of the shot-noise subthreshold voltage distribution can be obtained directly from the master equation (18) by taking voltage moments, as was done similarly for the diffusion approximation in Sec. III. Again, it proves convenient to take the moments with respect to $v = V - E$, yielding the relation

$$0 = \mathcal{R}_e(1-b_e)^m \left\langle \left(v + \frac{b_e \mathcal{E}_e}{1-b_e} \right)^m \right\rangle - \mathcal{R}_e \langle v^m \rangle + \mathcal{R}_i (1-b_i)^m \left\langle \left(v + \frac{b_i \mathcal{E}_i}{1-b_i} \right)^m \right\rangle - \mathcal{R}_i \langle v^m \rangle + \frac{m}{\tau_L} (\mathcal{E}_L \langle v^{m-1} \rangle - \langle v^m \rangle), \tag{19}$$

where $\mathcal{E}_L = E_L - E$. From this equation it can be shown that the mean voltage is equal to E and the variance σ^2 is identical to σ_D^2 given in Eq. (15): the diffusion approximation as formulated in Sec. III gives the first two moments exactly as was seen in the top two panels of Figs. 2(a)–2(c).

The third central moment can be written

$$\langle v^3 \rangle = \frac{\tau_L}{3} \frac{\mathcal{R}_e b_e^3 \mathcal{E}_e^3 + \mathcal{R}_i b_i^3 \mathcal{E}_i^3}{1 + \mathcal{R}_e \tau_L b_e (1 - b_e + b_e^2/3) + \mathcal{R}_i \tau_L b_i (1 - b_i + b_i^2/3)} - \tau_L \frac{\langle v^2 \rangle (\mathcal{R}_e b_e^2 \mathcal{E}_e (2 - b_e) + \mathcal{R}_i b_i^2 \mathcal{E}_i (2 - b_i))}{1 + \mathcal{R}_e \tau_L b_e (1 - b_e + b_e^2/3) + \mathcal{R}_i \tau_L b_i (1 - b_i + b_i^2/3)}, \tag{20}$$

which can be used to obtain the skew $\mathcal{S} = \langle v^3 \rangle / \sigma^3$ exactly. To give a transparent comparison with the prediction of the skew for the diffusion approximation $\mathcal{S}_D$, the case of a purely excitatory drive is again considered. In this case the skew becomes

$$\mathcal{S} = \frac{1 - \tau_L \mathcal{R}_e b_e (2 - b_e)}{1 + \tau_L \mathcal{R}_e b_e (1 - b_e + b_e^2/3)} \sqrt{\frac{8[1 + \tau_L \mathcal{R}_e b_e (1 - b_e/2)]}{9 \tau_L \mathcal{R}_e}}, \tag{21}$$

which in the diffusion limit, i.e., b_e small but with $\mathcal{R}_e \tau_L b_e$ held constant, the skew simplifies to

$$\mathcal{S} \simeq \frac{1 - 2\tau_L \mathcal{R}_e b_e}{1 + \tau_L \mathcal{R}_e b_e} \sqrt{\frac{8 b_e (1 + \tau_L \mathcal{R}_e b_e)}{9 \tau_L \mathcal{R}_e b_e}} \sim \sqrt{b_e}. \tag{22}$$

For $2\tau_L \mathcal{R}_e b_e < 1$ this skew is positive and clearly different from that calculated from the Fokker-Planck equation (17), which is negative. A comparison of the diffusion-level skew and full skew is given in Fig. 2 for different values of $\tau_L \mathcal{R}_e b_e$ as b_e is varied (this choice ensures that the mean voltage E remains constant). Data from simulations are also provided

with the exact results to underline the fact that approaches that use simulations in which Poissonian fluctuations are replaced by Gaussian white noise will also be in error at the level of the skew.

C. Consistent expansions of the master equation

The master equation can be expanded directly in powers of b_e with $\tau_L \mathcal{R}_e b_e$ held constant to ensure a constant mean E. The term of Eq. (18) that deals with excitatory pulses can be expanded to second order in b_e to yield

$$\frac{1}{1-b_e}P\left(\frac{V-b_eE_e}{1-b_e}\right)-P(V) = b_eP(V)+b_e(V-E_e)\frac{\partial P(V)}{\partial V} + \frac{b_e^2}{2}\frac{\partial^2}{\partial V^2}[(V-E_e)^2P(V)]+O(b_e^3). \tag{23}$$

On inserting this expansion, and the equivalent for inhibition, into the master equation (18), it is straightforward to show that the Fokker-Planck equation (12) is obtained. Hence in this expansion the mean and variance are given correctly, whereas the skew is given incorrectly. This is, of course, not too surprising: though there are some contributions to the skew at second order arising from the multiplicative noise, there are also terms missed that come from the higher-order terms dropped in the truncation of the expansion (23).

For a consistent solution it would be better to derive a systematic expansion that gives the moments correctly order by order in b_e. For the steady-state subthreshold distribution, centered around E, this can be achieved by writing the equation in a dimensionless variable $y=(V-E)/\sigma$. This removes the implicit b_e, b_i scale in $V-E$. The expansion analogous to (23) for the distribution $f(y)$ to order b_e yields

$$b_e\frac{\partial}{\partial y}(fy)-\frac{b_e\mathcal{E}_e}{\sigma}\frac{\partial f}{\partial y}+\frac{1}{2}\frac{b_e^2\mathcal{E}_e^2}{\sigma}\frac{\partial^2 f}{\partial y^2}, \tag{24}$$

where it should be noted that $b_e/\sigma \sim \sqrt{b_e}$. Together with the rest of the master equation, this yields

$$\tau\frac{\partial f_0}{\partial t}=\frac{\partial^2 f_0}{\partial y^2}+\frac{\partial}{\partial y}(f_0 y) \tag{25}$$

at zero order. The steady-state solution in terms of the voltage V is a Gaussian of mean E and variance σ given by Eqs. (10) and (15) and with vanishing skew. In comparison with the Fokker-Planck equation (12), it can be shown that Eq. (25) is identical to that of the diffusion approximation except that in the argument of the second derivative of Eq. (12) the voltage in the quadratic term has been replaced by its average value E.

A heuristic way of arriving at this approximation is to expand the synaptic drive given in Eq. (2). Considering just the excitatory component, the conductance can be first expanded into tonic g_{e0} and fluctuating g_{eF} components:

$$g_e(V-E_e)=g_{e0}(V-E_e)+g_{eF}(V-E_e). \tag{26}$$

The first term on the right-hand side is absorbed directly into the leak conductance, leading to the effective time constant τ and reversal potential E. The second term on the right-hand side represents the noise. This noise term can be expanded around the average voltage E to give

$$g_{eF}(V-E_e)=g_{eF}(E-E_e)+g_{eF}(V-E). \tag{27}$$

In terms of the variable $V-E$, which measures the difference of the voltage from its mean, the expansion on the right-hand side represents additive and multiplicative components, respectively. If the amplitude of g_{eF} is zero, then $V-E=0$. Hence, if g_{eF} is small, the multiplicative term must be less significant than the additive term. Keeping the leading-order additive fluctuations and dropping the multiplicative term yields an approximation for the synaptic drive that comprises a tonic conductance with additive current-based noise. In the diffusion approximation this results in a Fokker-Planck equation equivalent to that given in Eq. (25). This approximation has been used previously under the name of the "effective time constant" or "Gaussian approximation"[12,26,39–42] and can be justified [via Eq. (24)] as the leading term in the expansion of the master equation (18). Moreover, it allows for a perturbative approach for calculating the skew by expanding to higher order, as was shown recently for a filtered synaptic drive.[6]

D. Voltage distribution for excitatory shot noise

For the case of combined excitation and inhibition, an analytic solution of Eq. (18) appears difficult. However, in the absence of inhibition a solution can be found using a generalization of a standard method[38] developed for Poissonian shot noise. This recursive approach, which has been used previously[30,33] in the context of neuronal firing rates, is now reviewed.

In the absence of inhibition the dynamics are governed by the relaxation, due to the leak conductance, and the excitatory jumps. The recursive method breaks the voltage range into a number of segments that can be solved successively. The first segment is between the leak potential E_L and the voltage $V_1=E_L+b_e(E_e-E_L)$ to which an excitatory jump brings the neuron from this leak potential. The dynamics in this segment are governed purely by the relaxation and the excitatory jumps out. The probability distribution within the segment P_{01}, between $V_0=E_L$ and V_1, therefore obeys

$$\tau_L\mathcal{R}_eP_{01}=\frac{\partial}{\partial V}[(V-E_L)P_{01}] \tag{28}$$

and has the solution

$$P_{01}=A(V-E_L)^{\tau_L\mathcal{R}_e-1}, \tag{29}$$

where A is a constant to be determined by normalization. For cases of moderate rate and higher $\tau_L\mathcal{R}_e>0$, the distribution vanishes at $V=E_L$. The distribution P_{12} between V_1 and V_2 can now be calculated using (18), where V_2 is the voltage that an excitatory jump takes the neuron to V_1. Clearly, this can be continued for arbitrary ranges V_k to V_{k+1}, where V_k

$=E_e-(E_e-E_L)(1-b_e)^k$ and the voltage distribution $P_{k,k+1}$ satisfies

$$P_{k,k+1}=P_{k-1,k}(V_k)\left(\frac{V-E_L}{V_k-E_L}\right)^{\tau_L\mathcal{R}_e-1}-\frac{\tau_L\mathcal{R}_e}{1-b_e}\int_{V_k}^{V}\frac{dW}{W-E_L}\left(\frac{V-E_L}{W-E_L}\right)^{\tau_L\mathcal{R}_e-1}\times P_{k-1,k}\left(\frac{W-b_eE_e}{1-b_e}\right). \tag{30}$$

This method is best suited for cases in which the probability density is dominated by the first few segments. If this is not the case, the necessity of calculating the integrals (30) numerically makes a more direct numerical approach desirable. However, this uniamplitude case is rather artificial; as can be seen in Fig. 1(c), even for the case where inhibition is present, there is a discontinuity in the gradient of the distribution. This is an artifact that is not present if the more biologically realistic case of a distribution of synaptic amplitudes is considered.

E. Shot noise with amplitude distributions

In the previous section the uniamplitude synapse was employed to illustrate the differences between the shot-noise dynamics and the diffusion approximation. The more general case of an amplitude distribution, for which pulses within an amplitude range $b_e\to b_e+db_e$ arrive at a rate density $\rho_e(b_e)$, is now examined.

From a direct generalization of the argument that lead to Eq. (18) the master equation comprising an amplitude distribution can be written

$$\frac{\partial}{\partial t}P(V)=\int_0^1 db_e\left[\frac{1}{1-b_e}P\left(\frac{V-b_eE_e}{1-b_e}\right)-P(V)\right]\rho_e(b_e)+\int_0^1 db_i\left[\frac{1}{1-b_i}P\left(\frac{V-b_iE_i}{1-b_i}\right)-P(V)\right]\rho_i(b_i)+\frac{1}{\tau_L}\frac{\partial}{\partial V}[(V-E_L)P(V)], \tag{31}$$

where the integral of the rate density ρ_e over the range of b_e yields the net rate of pulses $\mathcal{R}_e$. The approach used to calculate the moments of the distribution [Eq. (19)] is identical to the previous section. Using the definition

$$\overline{b_e^m}=\frac{1}{\mathcal{R}_e}\int_0^1 db_e b_e^m\rho(b_e), \tag{32}$$

and similarly for $\overline{b_i^m}$, the following results for the mean and variance are found:

$$\langle V\rangle=\frac{E_L+E_e\tau_L\mathcal{R}_e\overline{b_e}+E_i\tau_L\mathcal{R}_i\overline{b_i}}{1+\tau_L\mathcal{R}_e\overline{b_e}+\tau_L\mathcal{R}_i\overline{b_i}}, \tag{33}$$

$$\sigma^2=\frac{\tau_L}{2}\frac{\mathcal{R}_e\overline{b_e^2}\mathcal{E}_e^2+\mathcal{R}_i\overline{b_i^2}\mathcal{E}_i^2}{[1+\tau_L\mathcal{R}_e(\overline{b_e}-\overline{b_e^2}/2)+\tau_L\mathcal{R}_i(\overline{b_i}-\overline{b_i^2}/2)]}. \tag{34}$$

It can be seen that the variance is identical in form to Eq. (15), which is also the exact shot-noise variance for a uniamplitude distribution, except that the b_e^m forms in the numerator and denominator have been replaced by $\overline{b_e^m}$. Furthermore, by inserting the expansion (23) into Eq. (31) the corresponding Fokker-Planck equation can be derived, which is identical in form to the case (12) except that again the quantities b_e^m and b_i^m are replaced by their expectations.

The skew for this case also follows accordingly from Eq. (20). In the absence of inhibition this skew can be written

$$\mathcal{S}=\frac{\overline{b_e^3}}{\overline{b_e^2}^{3/2}}\frac{1-\tau_L\mathcal{R}_e(3\overline{b_e^2}^2/\overline{b_e^3}-\overline{b_e}-\overline{b_e^2})}{1+\tau_L\mathcal{R}_e(\overline{b_e}-\overline{b_e^2}+\overline{b_e^3}/3)}\times\sqrt{\frac{1+\tau_L\mathcal{R}_e(\overline{b_e}-\overline{b_e^2}/2)}{9\tau_L\mathcal{R}_e/8}}. \tag{35}$$

A specific choice for the amplitude distribution will be considered below. However, it should be noted that the prefactor of Eq. (35) allows for the skew to be stronger than the uniamplitude case.

1. Numerical solution for the excitation-only distribution

The recursion solution of the Gilbert and Pollak form[38] reviewed in the previous section is clearly not appropriate for the case of an amplitude distribution. An efficient numerical method[31] has been developed for master equations of the form (31) in which both excitation and inhibition are present. However, here the case of excitation only will be considered for which the following elementary numerical scheme can be used to find the steady-state density.

By replacing the integral over b_e in Eq. (31) by an integral over the corresponding voltage, the master equation can be written

$$0=\int_{E_L}^{V}\frac{dWP(W)}{E_e-W}\tau_L\rho_e\left(\frac{W-V}{W-E_e}\right)+(1-\tau_L\mathcal{R}_e)P(V)+(V-E_L)\frac{\partial P(V)}{\partial V}. \tag{36}$$

The voltage range is now discretized over a lattice $V_k=E_L+k\Delta_V$ with lattice constant Δ_V [please note that this definition of V_k differs from that used previously in the context of uniamplitude distributions near Eq. (28)]. With the probability density P_k evaluated on these lattice points, the corresponding difference equation, valid for $k\geqslant 1$, can be written as

$$P_{k+1}=P_k+\frac{\Delta_V}{V_k-E_L}[(\mathcal{R}_e\tau_L-1)P_k-\Sigma_k], \tag{37}$$

with the integral in Eq. (36) approximated by

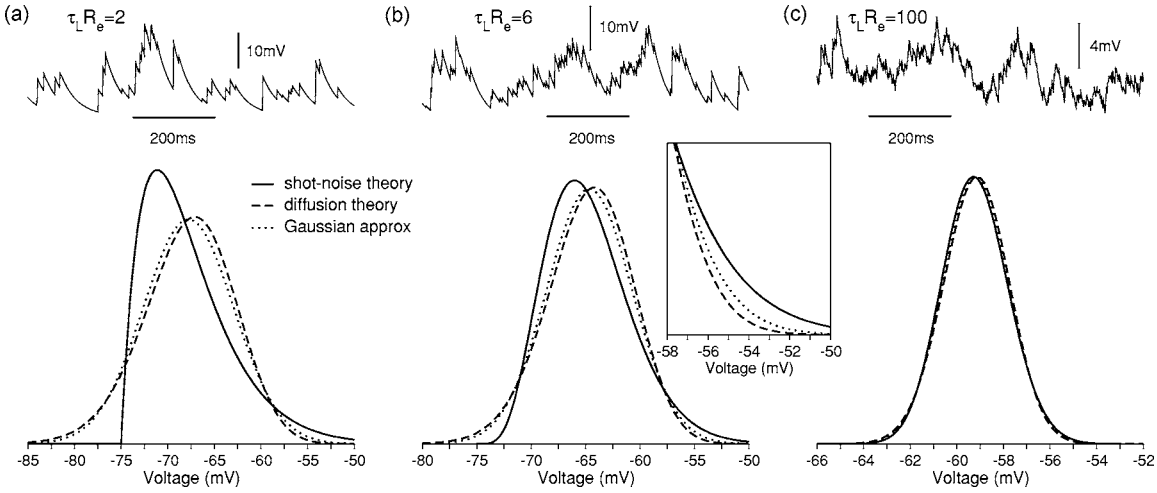

FIG. 3. Comparison of shot-noise, diffusion-level, and Gaussian-approximation voltage densities for neurons receiving synapses with a distribution of amplitudes. The upper panels show example voltage trajectories for each case, where from (a) to (c), the dynamics becomes more diffusive and less shot-like. (a) Large-amplitude shot noise; $\mathcal{R}_e$=0.1 kHz, $\overline{b_e}$=0.0533 giving mean pulse amplitudes of 4 mV from the leak potential E_L. The Gaussian approximation gives a slightly better account of the full distribution, which is positively skewed, than the diffusion approximation does, which itself is negatively skewed. (b) Moderate-amplitude shot noise; $\mathcal{R}_e$=0.3 kHz, $\overline{b_e}$=0.0267 giving mean pulse amplitudes of 2 mV from the leak potential E_L. Again the full distribution shows a significant positive skew. As can be seen in the inset, the diffusion approximation, and to a lesser extent, the Gaussian approximation underestimate the probability density for $V>-55$ mV. Despite being at the tail of this distribution, this difference could potentially cause a significant error for estimations of the firing rate of neurons in the presence of a threshold for the generation of outgoing action potentials, which is typically set in the range $V=-55$ to -50 mV. (c) Low-amplitude shot noise; $\mathcal{R}_e$=5 kHz, $\overline{b_e}$=0.00267 giving mean pulse amplitudes of 0.2 mV from the reversal leak E_L. In this high-rate case corresponding to the diffusion limit, both the diffusion approximation and the full shot-noise distribution approach the Gaussian approximation. For all cases, the shot-noise distribution was calculated using the numerical scheme given in Eq. (37) with the leak potential set at $E_L=-75$ mV and with τ_L=20 ms.

$$\Sigma_k = \sum_{j=1}^{k} \frac{P_j \Delta_V}{E_e - V_j} \tau_L \rho_e\left(\frac{V_k - V_j}{E_e - V_j}\right) - \frac{P_k \Delta_V}{E_e - V_k} \frac{\tau_L}{2} \rho_e(0), \qquad (38)$$

and with the boundary conditions $P(E_L)=P_0=0$ and $P_1=1$; the normalization is enforced after the integration (37) is complete.

2. An exponential distribution of amplitudes

A specific choice for the synaptic amplitude distribution is now considered for which b_e is exponentially distributed. Given that b_e has an upper bound of 1, a cutoff has to be enforced. However, for mean values $\overline{b_e} \ll 1$ this cutoff can be neglected and the approximation $\rho_e = \mathcal{R}_e \exp(-b_e/\overline{b_e})/\overline{b_e}$ is a good one. Assuming this approximation to hold, the expectations of the second and third powers of b_e are

$$\overline{b_e^2} = 2\overline{b_e}^2 \quad \text{and} \quad \overline{b_e^3} = 6\overline{b_e}^3. \qquad (39)$$

Because the exponential distribution has a tail, it can be expected that the skew is correspondingly stronger than that for the uniamplitude distribution considered in a previous section. To compare these two skews the quantities (39) are inserted into Eq. (35) and terms of order $\mathcal{R}_e \overline{b_e}^2$ or higher dropped. The resulting form of the skew, written in terms of the mean $\overline{b_e}$, is

$$\mathcal{S} \simeq \frac{3}{\sqrt{2}} \frac{1 - \tau_L \mathcal{R}_e \overline{b_e}}{1 + \tau_L \mathcal{R}_e \overline{b_e}} \sqrt{\frac{8\overline{b_e}(1 + \tau_L \mathcal{R}_e \overline{b_e})}{9\tau_L \mathcal{R}_e \overline{b_e}}}. \qquad (40)$$

In comparison with Eq. (22), it can be seen that this skew is stronger and has a larger range of positivity than that derived for the uniamplitude distribution: the effect of the positive skew is yet more enhanced for biologically realistic distributions.

In Fig. 3 subthreshold voltage densities are plotted for the amplitude-distributed shot-noise dynamics and the corresponding diffusion and Gaussian approximations [these are obtained by appropriately replacing b_e and b_e^2 in Eqs. (7), (8), and (24) by their expectations]. As can be seen clearly in Figs. 3(a) and 3(b), the full shot-noise distribution is significantly positively skewed (peak to the left of the mean with a tail extending to the right). In the detail of the distribution in Fig. 3(b) it should be noted that the Gaussian approximation—the zero-order expansion of the master equation—provides a slightly better approximation to the correct dynamics than the negatively skewed diffusion approximation does. For Fig. 3(c), which shows a case in which the diffusion approximation is expected to be good ($\mathcal{R}_e \tau_L = 80$), all distributions approach the Gaussian form.

V. CONCLUSION

The shot-noise dynamics of the subthreshold voltage of neurons subject to a barrage of synaptic input was considered. A number of results and methods existing in the literature were reviewed and new, exact results for the voltage moments derived. The role of shot noise as the cause of the positive skew of the distribution, with a peak to the left of the voltage mean and a long tail to the right, was emphasized and the weakness of the diffusion approximation identified: specifically its crossing of the inhibitory boundary and its prediction of a negative skew. An expansion of the corresponding master equation was also developed, the zero-order of which predicts a Gaussian distribution for the voltage. For the subthreshold case this gives a better indication of the

distribution than the diffusion approximation does and allows for higher-order moments to be obtained systematically via a perturbation expansion, both for unfiltered and filtered[6] shot-noise drives. It should be noted that in this approach the voltage is expanded around its mean subthreshold value: for firing neurons care must be taken in using the Gaussian approximation as the mean voltage is shifted away from this value by the imposition of a threshold for the generation of outgoing spikes.

As the skew is clearly a high-order effect, it is legitimate to question whether this detail has a measurable influence on the input-output properties of neurons beyond that predicted by the diffusion or Gaussian approximations. In Fig. 3 the full shot-noise distribution was shown to extend for voltages $V > -55$ mV. Though an analysis of the firing rate of neurons receiving synaptic shot noise is beyond the scope of this Focus Article, it should be noted that this voltage range is typical for action potential generation. So, though the skew is indeed a high-order feature that affects mostly the tail of the distribution, it can potentially have a significant effect on the firing rate of a neuron. This is consistent with results from a numerical study[31] in which the difference in firing rate between the diffusion approximation and the full shot-noise dynamics were quoted at 15% for the case of excitatory jumps of 2 mV [as used here in Fig. 3(b)] and 30% for 4 mV jumps. A systematic analysis of the role of shot noise and its related skew in the generation of action potentials, which is currently lacking in the literature, has the potential to provide further insight into the role of fluctuations in neuronal signaling.[43–45]

[1] D. W. Moran and A. B. Schwartz, J. Neurophysiol. **82**, 2676–2692 (1999).
[2] E. Todorov, Nat. Neurosci. **3**, 391–398 (2000).
[3] G. Silberberg, C. Z. Wu, and H. Markram, J. Physiol. (London) **556**, 19–27 (2004).
[4] S. Stroeve and S. Gielen, Neural Comput. **13**, 2005–2029 (2001).
[5] M. Rudolph, Z. Piwkowska, M. Badoual, T. Bal, and A. Destexhe, J. Neurophysiol. **91**, 2884–2896 (2004).
[6] M. J. E. Richardson and W. Gerstner, Neural Comput. **17**, 923–947 (2005).
[7] L. Lapicque, J. Physiol. Pathol. Gen. **9**, 620–635 (1907).
[8] R. B. Stein, Biophys. J. **7**, 37–68 (1967).
[9] P. I. M. Johannesma, in *Neural networks*, edited by E. R. Caianiello (Springer, New York, 1968), pp. 116–144.
[10] H. C. Tuckwell, J. Theor. Biol. **77**, 65–81 (1979).
[11] W. J. Wilbur and J. Rinzel, J. Theor. Biol. **105**, 345–386 (1983).
[12] P. Lansky and V. Lanska, Biol. Cybern. **56**, 19–26 (1987).
[13] A. Kamondi, L. Acsady, X.-J. Wang, and G. Buzsaki, Hippocampus **8**, 244–261 (1998).
[14] A. Destexhe and D. Paré, J. Neurophysiol. **81**, 1531–1547 (1999).
[15] M. V. Sanchez-Vives and D. A. McCormick, Nat. Neurosci. **3**, 1027–1034 (2000).
[16] C. Monier, F. Chavane, P. Baudot, L. J. Graham, and Y. Frégnac, Neuron **37**, 663–680 (2003).
[17] C. Holmgren, T. Harkany, B. Svennenfors, and Y. Zilberter, J. Physiol. (London) **551**, 139–153 (2003).
[18] F. S. Chance, L. F. Abbott, and A. D. Reyes, Neuron **35**, 773–782 (2002).
[19] A. N. Burkitt, H. Meffin, and D. B. Grayden, Biol. Cybern. **89**, 119–125 (2003).
[20] A. Destexhe, M. Rudolph, and D. Paré, Nat. Rev. Neurosci. **4**, 739–751 (2003).
[21] J.-M. Fellous, M. Rudolph, A. Destexhe, and T. J. Sejnowski, Neuroscience (Oxford) **122**, 811–829 (2003).
[22] S. A. Prescott and Y. De Koninck, Proc. Natl. Acad. Sci. U.S.A. **100**, 2076–2081 (2003).
[23] L. A. Grande, G. A. Kinney, G. L. Miracle, and W. J. Spain, J. Neurosci. **24**, 1839–1851 (2004).
[24] A. Kuhn, A. Aertsen, and S. Rotter, J. Neurosci. **24**, 2345–2356 (2004).
[25] M. Rudolph and A. Destexhe, Neural Comput. **15**, 2577–2618 (2003).
[26] M. J. E. Richardson, Phys. Rev. E **69**, 051918 (2004).
[27] M. Rudolph and A. Destexhe, Neural Comput. **17**, 2301–2315 (2005).
[28] B. Lindner and A. Longtin, Neural Comput. (to be published).
[29] R. Moreno-Bote and N. Parga, Phys. Rev. Lett. **94**, 088103 (2005).
[30] H. C. Tuckwell, *Introduction To Theoretical Neurobiology* (Cambridge University Press, Cambridge, 1988), Vol. 2.
[31] D. Q. Nykamp and D. Tranchina, J. Comput. Neurosci. **8**, 19–50 (2000).
[32] N. Hohn and A. N. Burkitt, Phys. Rev. E **63**, 031902 (2001).
[33] A. Kuhn, A. Aertsen, and S. Rotter, Neural Comput. **15**, 67–101 (2003).
[34] B. Lindner, Phys. Rev. E **73**, 022901 (2006).
[35] R. Moreno, J. de la Rocha, A. Renart, and N. Parga, Phys. Rev. Lett. **89**, 288101 (2002).
[36] M. Musila and P. Lansky, Int. J. Bio-Med. Comput. **31**, 233–245 (1992).
[37] H. Risken, *The Fokker-Planck Equation* (Springer, Berlin, 1996).
[38] E. N. Gilbert and H. O. Pollak, Bell Syst. Tech. J. **39**, 333–350 (1960).
[39] A. Manwani and C. Koch, Neural Comput. **11**, 1797–1829 (1999).
[40] A. N. Burkitt and G. M. Clark, Neurocomputing **26–27**, 93–99 (1999).
[41] A. N. Burkitt, Biol. Cybern. **85**, 247–255 (2001).
[42] G. La Camera, W. Senn, and S. Fusi, Neurocomputing **58**, 253–258 (2004).
[43] B. Lindner and L. Schimansky-Geier, Phys. Rev. Lett. **86**, 2934–2937 (2001).
[44] G. Silberberg, M. Bethge, H. Markram, K. Pawelzik, and M. Tsodyks, J. Neurophysiol. **91**, 704–709 (2004).
[45] N. Fourcaud-Trocme and N. Brunel, J. Comput. Neurosci. **18**, 311–321 (2005).